Systems Genetics Analysis of a Recombinant Inbred Mouse Cell Culture Panel Reveals Wnt Pathway Member Lrp6 as a Regulator of Adult Hippocampal Precursor Cell Proliferation

Suresh Kannan, Zeina Nicola, Rupert W. Overall, Muhammad Ichwan, Gerardo Ramírez-Rodríguez, Anna N. Grzyb, Giannino Patone, Kathrin Saar, Norbert Hübner, Gerd Kempermann

STEM CELLS

TISSUE-SPECIFIC STEM CELLS

Systems Genetics Analysis of a Recombinant Inbred Mouse Cell Culture Panel Reveals Wnt Pathway Member Lrp6 as a Regulator of Adult Hippocampal Precursor Cell Proliferation

SURESH KANNAN,[a,b] ZEINA NICOLA,[c] RUPERT W. OVERALL,[a] MUHAMMAD ICHWAN,[a] GERARDO RAMIREZ-RODRIGUEZ,[d] ANNA N. GRZYB,[c] GIANNINO PATONE,[e] KATHRIN SAAR,[e] NORBERT HÜBNER,[e] GERD KEMPERMANN[a,c]

[a]CRTD—Center for Regenerative Therapies Dresden, Technische Universität Dresden, Dresden, Germany; [b]Department of Biomedical Sciences, Sri Ramachandra University, Porur, Chennai, India; [c]German Center for Neurodegenerative Diseases (DZNE) Dresden, Dresden, Germany; [d]Laboratory of Neurogenesis, Division of Clinical Investigations, National Institute of Psychiatry "Ramón de la Fuente Muñiz," México D.F., México; [e]Max-Delbrück Center for Molecular Medicine, Berlin, Germany

Correspondence: Gerd Kempermann, Prof. Dr. med., German Center for Neurodegenerative Diseases (DZNE) Dresden, and CRTD-DFG Research Center for Regenerative Therapies Dresden, Fetscherstrasse 105, 01307 Dresden, Germany. Telephone: + 49 351 45882201; Fax: + 49 351 45882239; e-mail: gerd.kempermann@dzne.de

Received April 22, 2015; accepted for publication October 25, 2015; first published online in STEM CELLS *EXPRESS* February 3, 2016.

1066-5099/2016/$30.00/0

http://dx.doi.org/10.1002/stem.2313

Key Words. Adult stem cells • Dentate gyrus • Systems biology • Cells • Cultured • Quantitative trait loci • Lrp6 protein • Mouse

ABSTRACT

In much animal research, genetic variation is rather avoided than used as a powerful tool to identify key regulatory genes in complex phenotypes. Adult hippocampal neurogenesis is one such highly complex polygenic trait, for which the understanding of the molecular basis is fragmented and incomplete, and for which novel genetic approaches are needed. In this study, we aimed at marrying the power of the BXD panel, a mouse genetic reference population, with the flexibility of a cell culture model of adult neural precursor proliferation and differentiation. We established adult-derived hippocampal precursor cell cultures from 20 strains of the BXD panel, including the parental strains C57BL/6J and DBA/2J. The rates of cell proliferation and neuronal differentiation were measured, and transcriptional profiles were obtained from proliferating cultures. Together with the published genotypes of all lines, these data allowed a novel systems genetics analysis combining quantitative trait locus analysis with transcript expression correlation at a cellular level to identify genes linked with the differences in proliferation. In a proof-of-principle analysis, we identified *Lrp6*, the gene encoding the coreceptor to Frizzled in the Wnt pathway, as a potential negative regulator of precursor proliferation. Overexpression and siRNA silencing confirmed the regulatory role of *Lrp6*. As well as adding to our knowledge of the pathway surrounding Wnt in adult hippocampal neurogenesis, this finding allows the new appreciation of a negative regulator within this system. In addition, the resource and associated methodology will allow the integration of regulatory mechanisms at a systems level. STEM CELLS *2016;34:674–684*

SIGNIFICANCE STATEMENT

Neural stem cells from the hippocampus of adult mice can be grown in culture where they are amenable to experimental manipulation. The proliferation of these cells, and their differentiation into mature cell types, is under complex genetic control. To discover genes regulating stem and precursor cell proliferation, we have established cultures from different strains of mice. We measured proliferation rates and transcript expression in each cell line and mapped these to existing genotypes. Using a novel systems genetics approach, we identified the Wnt pathway gene Lrp6 as a novel negative regulator of proliferation in these cells.

INTRODUCTION

Adult hippocampal neurogenesis, the continued production of new neurons in the dentate gyrus of many mammalian species, is a complex phenotype under multigenetic control. A pool of stem cells proliferates and gives rise to precursor cells, some of which mature into functional granule cell neurons via a number of defined stages [1]. To date, more than 200 genes have been assigned roles in this process [2], and evidence from systems genetics studies suggest there will be many more [3]. Previous studies have made clear that adult hippocampal neurogenesis is strongly regulated by the genetic background of the individual [3–6]. The relationship between genome and phenotype is also complex. Single gene studies can identify the contribution of individual genes but usually fail to put the result into a genomic context. This is particularly true for some core phenotypes, such as cell proliferation, which are affected by very large numbers of

genes. Genetic association studies that link trait variance to individual genetic loci or genes are a strategy commonly used in human population-based studies to identify candidate genes, but this approach is rarely applied to animal research. Genetic reference populations of mice, however, offer a model in which the genetic components of complex phenotypes can be isolated and analyzed. We here used a recombinant inbred (RI) panel—a set of inbred strains derived from inbreeding an initial cross between two parental strains. The resulting strains are homozygous at every locus and have, on average, a 50:50 mix of the two parental genomes. The BXD panel—the largest mammalian RI population currently available—is derived from a cross between two mouse strains, C57BL/6J and DBA/2J [7–9]. Among many other differences, these parentals are also characterized by very large baseline differences in adult hippocampal neurogenesis [3–6] making this an ideal system for the study of adult neurogenesis. The BXD panel is fully genotyped and the parental strains have both been sequenced, providing rich genomic information. Genotypic and phenotypic data for the BXD model are publicly available at http://www.genenetwork.org.

Although many factors influencing precursor cell proliferation and differentiation have been identified and tested in vivo, this is a laborious process relying on often coarse outcome measures and involving large numbers of treated or transgenic animals. This limits the number of candidate genes which may be investigated in a realistic time frame. An in vitro model can overcome some of these limitations and help identify and validate potential neurogenic regulators. The proliferating progenitor cells of the hippocampal dentate gyrus can be isolated and grown in culture conditions where they can be maintained over many generations without losing their neurogenic potential [10, 11]. This study combined the strengths of ex vivo experiments with the power of the BXD panel.

In order to identify precursor cell-intrinsic key genes relevant to the control of adult hippocampal neurogenesis, we established hippocampal neural precursor cell cultures from 20 strains of the BXD panel (including the parentals). The result is the only such renewable in vitro genomic mapping resource that we are aware of. The cultures have been phenotyped for basic in vitro traits of adult neural precursor cell activity, as well as transcript expression under proliferating conditions. These phenotypes were then used in a novel combination of genomic linkage (quantitative trait locus mapping) and transcript-trait correlation to identify potential factors regulating proliferative activity in vitro. We thereby identified *Lrp6* as a novel candidate and have confirmed its negative regulatory role in precursor cell proliferation in vitro.

Materials and Methods

Animals

The adult hippocampal precursor cell lines generated in this study were derived from mixed-sex pools of 8–10 mice from 20 strains from BXD recombinant inbred population, including the two progenitor strains, C57BL/6J and DBA/2J. The mice were bred at Harlan as part of the GeNeSys (German Network for Systems Genetics) consortium and were between 5 and 7 weeks of age at the time of dissection. Animal handling and all procedures during the experiment were in accordance with the local and federal regulations regarding animal welfare.

Extraction and Culture of Precursor Cells from BXD Mice

The isolation and culturing of adult hippocampal precursor cells were done as previously described [10, 11]. Briefly, the hippocampi were dissected and collected in ice cold Hank's buffered saline solution (HBSS). The tissue was minced with a surgical knife and digested in an enzymatic cocktail containing papain (2.5 U/ml), dispase (1 U/ml), and deoxyribonuclease (250 U/ml) for 30–40 minutes at 37°C. After digestion, samples were washed free of enzymes with HBSS and centrifuged in a 22% Percoll solution at 1,500 rpm for 15 minutes. After washing with phosphate-buffered saline (PBS), the enriched fraction of precursor cells was seeded onto culture dishes coated with poly-D-lysine (PDL; 10 μg/ml; Sigma, Munich, Germany, http://www.sigmaaldrich.com/germany.html) and laminin (5 μg/ml; Roche, Basel, Switzerland, http://www.roche-applied-science.com). Precursor cells were cultured in Neurobasal media supplemented with 2% B27 (Invitrogen, Carlsbad, CA, http://www.invitrogen.com), 1 × GlutaMAX (Life Technologies, Rockville, MD, http://www.lifetech.com), 20 ng/ml human basic fibroblast growth factor (bFGF; PeproTech, Rocky Hill, NJ, http://www.peprotech.com), and 20 ng/ml epidermal growth factor (EGF; PeproTech). Every 2 days, half of the culture medium was replaced with fresh medium. Precursor cells were passaged at approximately 80% confluence by treating with Accutase (PAA Laboratories, Linz, Austria, http://www.paa.at) for 2 minutes, and reseeded in PDL/laminin-coated dishes at a density of 10,000 cells per cm^2.

Differentiation was induced by a 5-day sequential growth factor withdrawal protocol [11] whereby cells growing under standard proliferation conditions (20 ng/ml each of bFGF and EGF) were switched first to medium without any EGF but with 5 ng/ml FGF for 2 days, and then maintained for three additional days in medium without growth factors. The neurons were identified with anti-MAP2 (an antibody against microtubule-associated protein 2) and astrocytes with anti-GFAP (glial fibrillary acidic protein).

Immunocytochemistry

Precursor cells were cultured on glass coverslips coated with PDL/laminin. Cells were harvested by fixing in ice cold 4 % formaldehyde solution. For 5-bromo-2′-deoxyuridine (BrdU) staining, cells were washed with Tris-buffered saline (TBS) and 0.9 % NaCl, and DNA was denatured with 1N HCl for 30 minutes at 37°C. For all stainings, cells were blocked for 1 hour in blocking solution containing 10% donkey serum and 0.2% Triton X-100 in PBS. Primary and secondary antibodies were prepared in blocking solution. Cellular monolayers were incubated with primary antibodies overnight at 4°C and the secondary antibodies at room temperature for 2 hours. The nuclei were labeled with Hoechst and the coverslips mounted onto glass slides for microscopic examination.

The following primary antibodies and concentrations were used: mouse monoclonal anti-Nestin (1:200; Cat. Nr. 611658, BD Biosciences, San Diego, http://www.bdbiosciences.com), rabbit polyclonal anti-GFAP (1:1,000; Cat. Nr. Z0334, DakoCytomation, Glostrup, Denmark, http://www.dakocytomation.com), rabbit polyclonal anti-SOX2 (1:400; Cat. Nr. AB5603, Chemicon International, Temecula, CA, http://www.chemicon.com), mouse monoclonal anti-MAP2 (1:1,000; Cat. Nr. M1406, Sigma), mouse monoclonal anti-O4 (1:400; Cat. Nr. MAB1326, R&D Systems, Minneapolis, http://www.rndsystems.com), rat monoclonal anti-BrdU (1:500;

Cat. Nr. OBT0030, AbD Serotec). The secondary antibodies, DyLight 488, 549, Cy3 (Jackson ImmunoResearch, West Grove, PA, http://www.jacksonimmuno.com) were used at the concentration of 1:250 for different primary antibodies.

Standard RT-PCR and quantitative RT-PCR

Total RNA was prepared using the Qiagen RNeasy kit (Qiagen, Hilden, Germany, http://www1.qiagen.com). The adherent cell cultures were washed once with PBS and then harvested by on-plate lysis with buffer RLT. Lysate was collected using a cell scraper and RNA extracted following the manufacturer's protocol, including the optional DNase step. The concentration and the purity of RNA were analyzed using a NanoDrop 1000 spectrophotometer (Thermo Scientific). For reverse transcription, 1 μg of RNA was used. The cDNA was prepared using Superscript II kit (Invitrogen) using oligo(dT) primers following the manufacturer's protocol. A cDNA negative reaction was also set up without addition of reverse transcriptase enzyme to ensure no genomic DNA contamination.

Quantitative real-time reverse transcriptase polymerase chain reaction (qRT-PCR) for Lrp6 was performed using a SYBR Green PCR Mix (Qiagen) following the manufacturer's protocol. Template cDNA was prepared as above and each reaction contained cDNA from 0.1 μg total RNA. Thermal cycling and fluorescence detection were carried on an Opticon 2 DNA Engine (MJ Research). Quantification was done using the $\Delta\Delta$Ct method after normalizing to the β-actin (*Actb*) housekeeping gene. Primer sequences for *Lrp6* were 5′-gagctggactgttatccaactg-3′ and 5′-cttca tacgaggacacagcatc-3′ and for *Actb* 5′-tgacccagatcatgtttgaga-3′ and 5′-ggagagcatagccctcgtag-3′.

Western Blot

For Western blot analysis, the cells were collected in a RIPA buffer (0.1% SDS, 0.25% sodium deoxycholate, 1% Nonidet P-40, 150 mM NaCl, 1 mM EDTA, 50 mM Tris-HCl pH 7.5) with protease inhibitor cocktail (P8340, 1:100, Sigma) and disrupted by sonication. The proteins were separated by SDS-PAGE on 4%–15% Mini-PROTEAN TGX precast gels (BioRad, Hercules, CA, http://www.bio-rad.com) and transferred to a nitrocellulose membranes. The membranes were blocked and then probed with antibodies against Lrp6 (pLrp6; 1:1,000; Cat. Nr. LS-B7381, LSBio) and the phosphorylated form of Lrp6 (1:1,000; Cat. Nr. 25685, Cell Signaling, Beverly, MA, http://www.cellsignal.com), and Gapdh (1:1,000; Cat. Nr. MAB374, Chemicon International) or β-Actin (1:1,000; Cat. Nr. sc-81178, Santa Cruz, Santa Cruz, CA, http://www.scbt.com) as an internal loading control. Protein bands were detected using a horseradish peroxidase/chemiluminescence system (ECL Western Blotting Substrate, Pierce, Rockford, IL, http://www.piercenet.com) and visualized on Hyperfilm ECL (Amersham, Piscataway, NJ, http://www.amersham.com).

Films were scanned and band intensities determined using ImageJ (http://imagej.nih.gov/ij/). Results are shown as the normalized difference from control (NDC) calculated by first normalizing to β-actin, and then to the mean of the control group using the formula (x − control)/control. Thus the mean treatment value is the fold increase or decrease from the control.

Gene Silencing and Overexpression

For the knockdown experiment, a pool of four different small interfering RNA (siRNA) sequences targeting mouse Lrp6 was used (ON-TARGETplus SMARTpool, Cat. No. L-040651-01-0005, Dharmacon). Cells derived from C57BL/6, one of the parental strains, were cultured for 24 hours in the plates before the addition of 50 nM siRNA together with transfection agent (DharmaFECT, Dharmacon) and thereafter incubated for a further 48 hours before harvesting.

For overexpression of Lrp6, the plasmid pCAGGS-mLRP6-HA, containing the full-length mouse Lrp6 cDNA and pMesd was used (kindly provided by Daniel Wehner and Dr. Gilbert Weidinger, Biotec, Dresden, Germanyhttp://www.biotec.tu-dresden.de/research/alumni/weidinger.html, recent address: http://www.uni-ulm.de/med/med-biomolbio/research-groups/weidinger/group-members-weidinger-lab.html). The identities of the plasmids were confirmed by sequencing. Proliferating cells derived from C57BL/6 were transfected with plasmid DNA (8 μg mLRP6; 6 μg pMesd) using the Amaxa nucleofector system (Lonza) with the programme A33. Control cultures were transfected with an equivalent total amount (14 μg) of pMesd alone. Cultures were grown for a further 48 hours before harvesting. Overexpression was confirmed both at the transcript and protein levels by qPCR and Western blot (Materials and Methods section).

Microarray Processing

Total RNA from three replicate cultures (at different passages) from each of the 20 strains was extracted as described above. RNA samples were amplified using the TotalPrep RNA Amplification Kit (Illumina) and hybridized to MouseWG-6 v2.0 Expression BeadChips (Illumina). Raw bead-level data were preprocessed with quantile normalization in R/Bioconductor using the package *beadarray* (version 1.16.0) [12]. This algorithm includes a log transformation. The array was reannotated by querying each probe sequence against the mm9 mouse genome using the BLAT algorithm (kindly supplied by Dr. Jim Kent; http://hgwdev.cse.ucsc.edu/~kent/exe/linux). The genomic position of probes returning a single hit was then used to assign the probe to an NCBI Entrez GeneID (genome and annotations retrieved from ftp://ftp.ncbi.nlm.nih.gov on June 20, 2011). Probes targeting the same GeneID were collapsed as means to yield data for 21,155 unique genes. All arrays passed the standard hybridization quality control checks, as described in the Illumina hybridization protocol, and the pairwise correlation (Pearson's r) between the three replicates for each strain were high (mean = 0.99, SD = 0.0042). The normalized and reannotated data used for analysis are available from GeneNetwork (http://www.genenetwork.org/webqtl/main.py?FormID=sharinginfo&GN_AccessionId=706), and the raw data have been deposited in the GEO repository (http://www.ncbi.nlm.nih.gov/geo/; accession: GSE71466).

Correlation and Quantitative Trait Locus Analysis

Quantitative trait locus (QTL) mapping was carried out using marker regression as implemented by the *QTLReaper* software (http://qtlreaper.sourceforge.net/). All 20 strains were used in mapping. The likelihood ratio statistic (LRS) was computed for each of 3,791 informative genomic markers (ftp://atlas.uthsc.edu/users/shared/Genenetwork/GN398/BXD.geno.txt), and a genome-wide significance threshold was calculated for each trait by permuting the genotypes and performing the whole genome scan 1,000 times to create a distribution of the highest LRS. Scores above the 95th percentile of this distribution were considered to be genome-wide significant. An expression *cis*-QTL was defined by an overlap between the genomic position of the gene and the flanking markers of the QTL.

Correlations between strain means of the proliferation phenotype or Lrp6 and each gene on the microarray were

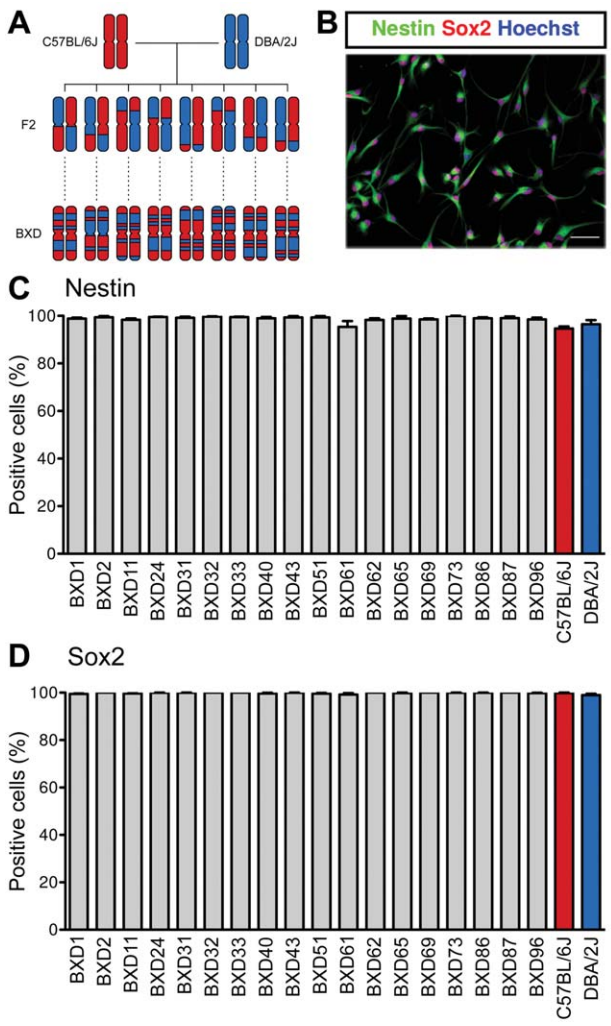

Figure 1. Creation of a genetic panel of proliferating neural precursor cultures from the adult hippocampus. The BXD panel has been derived from a cross of the mouse strains C57BL/6J (red) and DBA/2J (blue) and the F2 offspring subsequently inbred over many generations to produce a panel of homozygous lines each containing a unique mosaic of the parental genotypes **(A)**. Hippocampi were dissected from animals of the different strains, and the isolated precursor cells expanded in vitro to yield a resource of isogenic cell lines. The cultures were stained for the neural stem cell markers Nestin and Sox2 (a representative staining is shown in **B**). The proliferating cultures were at least 97% positive for Nestin **(C)** and Sox2 **(D)**. Graphs show means ± SEM. Red and blue bars indicate data for C57BL/6J and DBA/2J respectively. Scale bar in (B) = 50 μm.

calculated as Pearson's product-moment, and correlations with an absolute value of r smaller than .6 were discarded from further analysis. All calculations other than QTL mapping were performed using R/Bioconductor [13].

Statistics

Raw data are given as means and SEM. qPCR results are shown as $-\Delta\Delta C_t$ after normalization against an internal control. All t-tests were two-tailed Welch's tests assuming unequal variances.

Broad sense heritability was calculated for each phenotype as the variance of the strain means as a fraction of the total variance over all data points, that is, $\text{var}(m_x)/\text{var}(x)$ where x is the phenotype data and m_x represents the means of x for each strain. All statistics were calculated using R/Bioconductor [13].

Results

Characterization of Adult Hippocampal Precursor Cell Cultures from BXD Mice

For this study, cultures were established from 18 BXD lines as well as the two parental strains C57BL/6J and DBA/2J. We demonstrated the precursor cell nature of each culture by immunocytochemistry for two commonly used neural stem cell markers, Nestin and Sox2. We verified that a minimum of 97% cells were positive for both of these markers in all 20 cultured cell lines (Fig. 1). The multipotency of the cultured cells to generate neurons, astrocytes, and oligodendrocytes was confirmed after induction of differentiation by following a sequential growth factor withdrawal protocol (data not shown) as has been shown previously for these cells [10, 11]. This cryopreserved resource now offers a unique platform for repeated phenotyping of these strains in the context of the genetics of the BXD panel.

Differences in Proliferation and Differentiation Between Cell Lines

We quantified the rate of proliferation in the 20 BXD cultures. The cell proliferation rate was measured as the proportion of cells incorporating BrdU after 2 hours of labeling (Fig. 2A, 2B). Proportions ranged from 24.6% (BXD69) to 52.8% (BXD2), equating to more than twofold difference across the lines (Fig. 2C). Proliferation rates for the parental lines (C57BL/6J: 39.4%; DBA/2J: 38%) were close to the mean across all lines (mean: 36.7%; SD: 6.9%) indicating transgressive segregation of the proliferation phenotype (Fig. 2C)—evidence for the recombination of many small-effect alleles. Values for the proliferation rate also closely approximate a normal distribution (Fig. 2D)—further suggesting the presence of multiple genes contributing to the phenotype. Data were deposited in the GeneNetwork database (BXD RecordID: 17347).

Differentiation of the precursor cell cultures into a mixture of neurons and astrocytes was induced by sequential growth factor withdrawal. At the end of the differentiation period, the proportions of neurons and astrocytes formed by each line were counted by staining for Map2 and GFAP, respectively (Fig. 2E, 2I, 2F, 2J). Neuronal differentiation ranged from 8.9% to 36.4% (Fig. 2G), a four-fold difference among the extremes, even higher than observed for the proliferation traits. In the case of astrocytes, the values ranged from 42.6% to 85.7% (Fig. 2K), a little over twofold difference. Note that, because oligodendrocytes make up only a very small percentage of the differentiated progeny in this culture model (1%; Babu et al., [11]), it was not possible to reliably quantify an oligodendrocyte phenotype. Again, the parental lines exhibited values close to the mean for neuronal differentiation phenotype (C57BL/6J: 18.2%; DBA/2J: 17.8%; mean: 16.4%; SD: 5.9%; Fig. 2G) and astrocyte differentiation (C57BL/6J: 62.3%; DBA/2J: 68.4%; mean: 69.5%; SD: 8.7%; Fig. 2K). The normality quantile plots indicated a good fit to a normal distribution, albeit with some outliers (BXD86 for neurons and BXD96 for astrocytes) deviating from this trend (Fig. 2H, 2L).

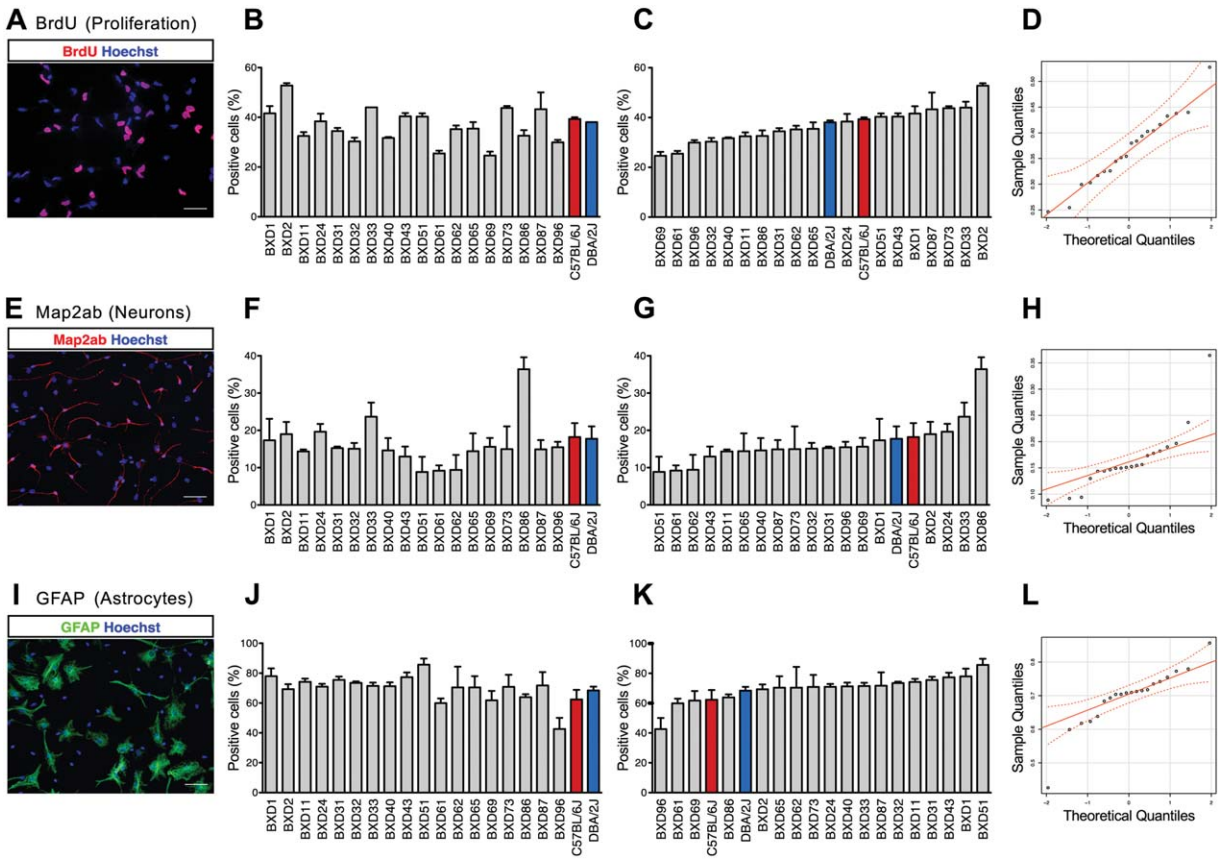

Figure 2. Characteristics of proliferation and differentiation vary across strains. The proliferative ability **(A–D)** and differentiation into neurons **(E–F)** or astrocytes **(I–L)** exhibited strong variation in the different strain measured. Results in (E–L) were measured after growth factor withdrawal (Materials and Methods section for details). Representative micrographs are shown of the cultures stained with antibodies against BrdU (2 hours after application, measuring actively dividing cells; A), Map2 (early neurons; E) and GFAP (astrocytes; I). Plots showing the percentage of cells staining with each marker are shown ordered by strain (B, F, J) and from lowest to highest (C, G, K). Parental strains are shown in red (C57BL/6J) or blue (DBA/2J). Normality plots for each trait include a least squares linear model (red line) for comparison (D, H, L). Scale bars in (A, E, I) = 50 μm. Abbreviations: BrdU, 5-bromo-2′-deoxyuridine; GFAP, glial fibrillary acidic protein; MAP2, microtubule-associated protein 2.

Data were deposited in GeneNetwork as BXD RecordIDs 17348 (neurons) and 17349 (astrocytes).

Because genomic background was the only variable perturbed in this study, and due to the low variation inherent in the controlled cell culture environment, we expected high heritability of the measured traits—which was confirmed by broad sense heritability values of 0.83, 0.53, and 0.54 for proliferation, neuron, and astrocyte differentiation respectively. It is thus clear that these phenotypes are under strong genetic control and that our experimental set-up provides a suitable model for the identification of genes, or networks of genes, responsible for the regulation of neural precursor cell proliferation and differentiation.

Quantitative Trait Analysis for Neurogenic Parameters in BXD RI Strains

A key application of the BXD recombinant inbred lines is their use for QTL mapping. In this technique, the variation in a measured phenotype is correlated to variation in allele distribution across the BXD lines. A significant association is thus evidence for regulation of the phenotype by some gene at the corresponding allele locus. We carried out QTL mapping for the proliferation, neuronal, and astrocyte differentiation phenotypes and plotted the association as the LRS at 3,791 informative markers across the genome (Fig. 3; Materials and Methods section for details). At a genome-wide significance level of 0.05, there were no significant associations for any of the three phenotypes. This shows that no single genes have a dominating effect on the proliferation and differentiation of neural precursor cells but rather, corroborating the evidence above, suggests that the genetic control of these phenotypes might be due to the synergistic influences of numerous small-effect genes.

Whole-Genome Transcript Expression in Proliferating Cultured Precursor Cells

There are many points of regulation between a genomic variant and a downstream phenotype, including, for example, RNA stability, effects of noncoding RNAs, protein translation, and post-translational processing. In order to bridge this gap, we decided to also investigate mRNA transcript expression levels which are an easily measured intermediate between gene sequence and phenotype. To this end, we hybridized mRNA from three replicate cultures from each cell line under proliferation conditions to Illumina Mouse-6 microarrays. The resulting data were reannotated using an updated mapping

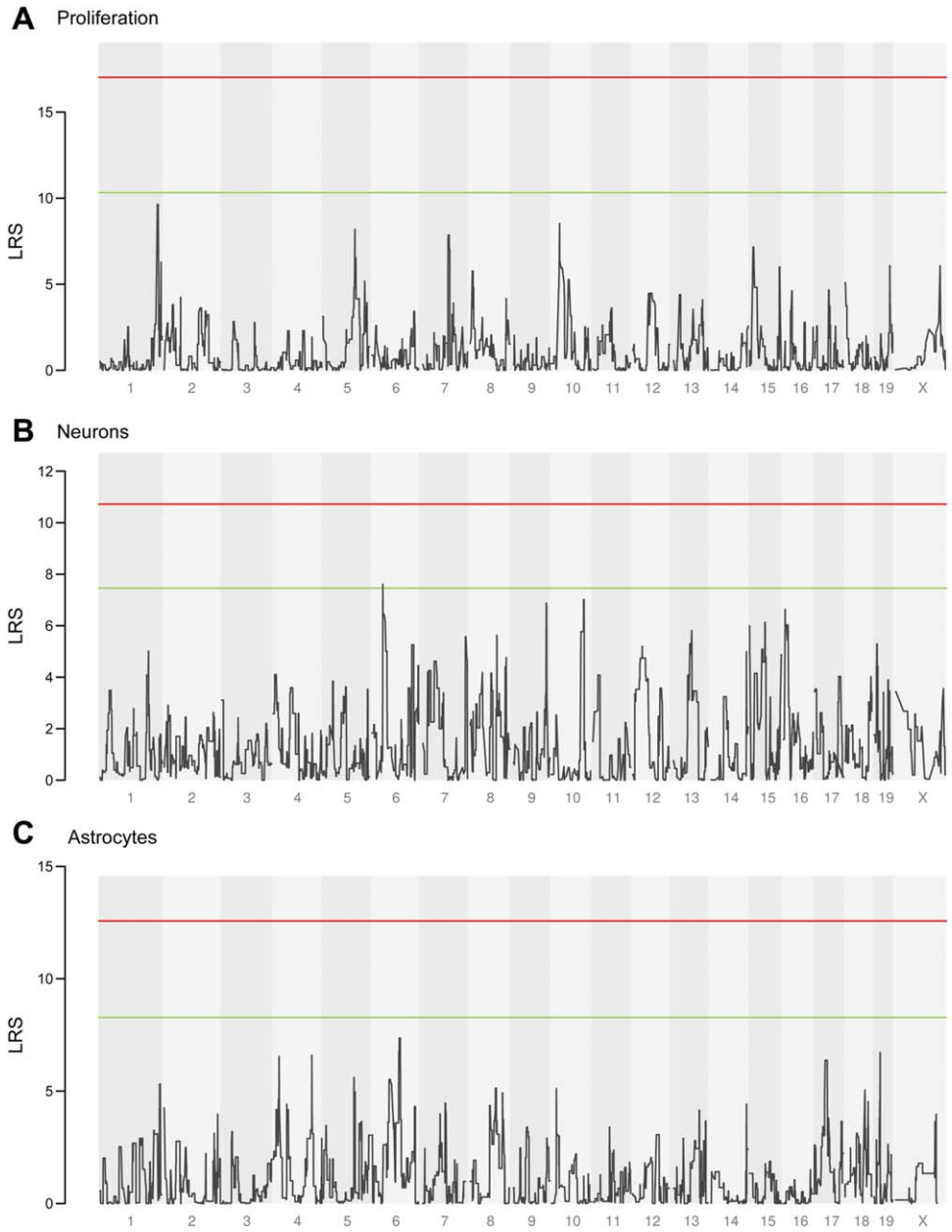

Figure 3. Genomic association plots do not reveal strong single-locus effects. Whole-genome quantitative trait locus mapping of the proliferation **(A)**, new neuron **(B)**, and astrocyte **(C)** traits did not detect any single genomic loci with a significant ($p < .05$ after genome-wide correction; red line) influence on trait expression. A less stringent threshold is also shown ($p < .63$, allowing one false positive per scan; green line). Abbreviation: LRS, likelihood ratio statistic.

(Materials and Methods section for details) to yield expression profiles for 21,155 unique genes across 20 precursor cell lines. The high genetic variation in these lines is evidenced by more than 200 transcripts showing a greater than 10-fold range in expression. Indeed, one gene, *Calca*, exhibits a more than 200-fold range in expression values and is associated with a *cis*-QTL with a likelihood ratio statistic (LRS) of 57. With higher expression from the DBA/2J allele and in the light of evidence that *Calca* expression can protect against kainic acid-induced neurotoxicity in the hippocampus [14], this finding may hint at an explanation for the increased sensitivity of the DBA/2J strain to kainic acid-induced seizures [15]. Genes such as this are prime candidates for further studies on the genetics of adult-derived hippocampal precursor cells. The expression profiles of all 21,155 genes from this study are publicly available from the GeneNetwork website (http://genenetwork.org) under the accession number GN706.

The *cis*-Acting Gene Lrp6 is Associated with Precursor Cell Proliferation

To link proliferation to gene expression, we calculated the Pearson correlation coefficient between the proliferation phenotype and each of the 21,155 genes represented on the arrays. Using a threshold of an absolute Pearson coefficient of 0.6 (i.e., strongly correlated or anticorrelated to the phenotype) we identified 1,092 transcripts whose expression patterns were similar to that

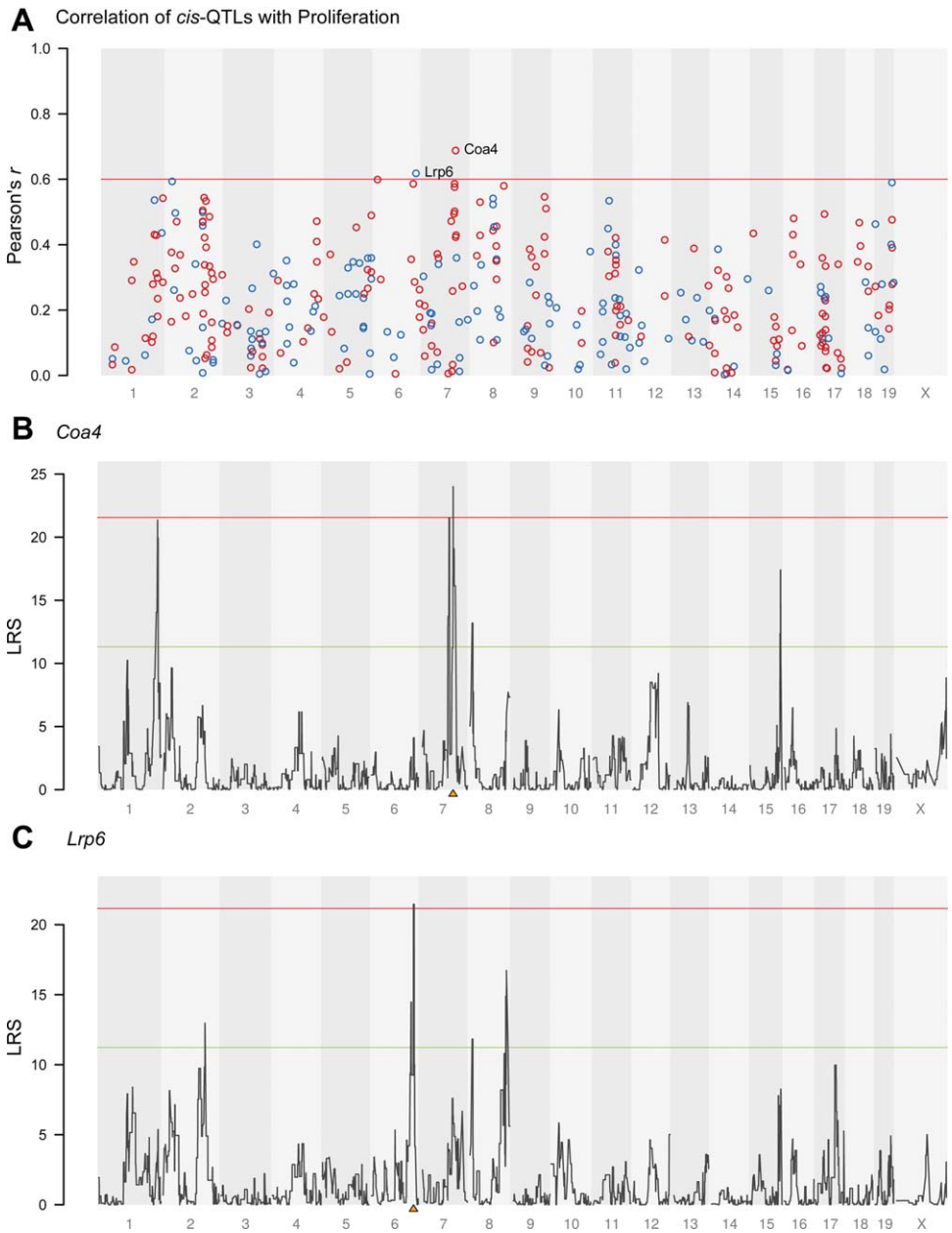

Figure 4. Incorporation of transcript expression data reveals two genes associated with precursor proliferation. The in vitro proliferation trait was correlated with whole-genome transcript expression profiles filtered for genes with a *cis*-QTL. Using a strict correlation threshold (absolute Pearson's $r > .6$), two candidate genes were identified, Coa4 and Lrp6 **(A)**. Genes where higher expression is associated with the C57BL/6J allele are shown in red, those with DBA/2-high expression are in blue. Genome-wide QTL plots show that both Coa4 **(B)** and Lrp6 **(C)** exhibit *cis*-QTLs. Orange triangles below each plot indicate the genomic position of the respective gene. Abbreviation: LRS, likelihood ratio statistic.

of the proliferation phenotype (Fig. 4A). Because of the polygenic nature of this phenotype, as noted earlier, many of these genes are likely not to be the actual sources of variation, but rather secondary effects mediated by other gene products. In this study, we were more interested in identifying those genes which play a causal role in the gene networks in which they are involved. The expression of such genes is expected to be tightly linked to the causal allelic variation—which can be detected by QTL mapping, as described above for the cellular phenotypes. A gene expression QTL can be classified as either a *cis*-QTL (where the associated polymorphism is in the same gene whose expression is being mapped) or a *trans*-QTL (where the polymorphism and gene are in different locations). The presence of a *cis*-QTL thus provides very strong evidence of a gene which plays a driving role in the regulation of its surrounding network of genes and their associated phenotypes.

We identified two *cis*-QTLs within the list of correlating transcripts, *Coa4* ("cytochrome c oxidase assembly factor 4"; $r = .69$; Fig. 4B) and *Lrp6* ("low density lipoprotein receptor-related protein 6" $r = -.62$; Fig. 4C).

Searches of other BXD expression databases of whole hippocampal tissue could not detect significant *cis*-QTLs for

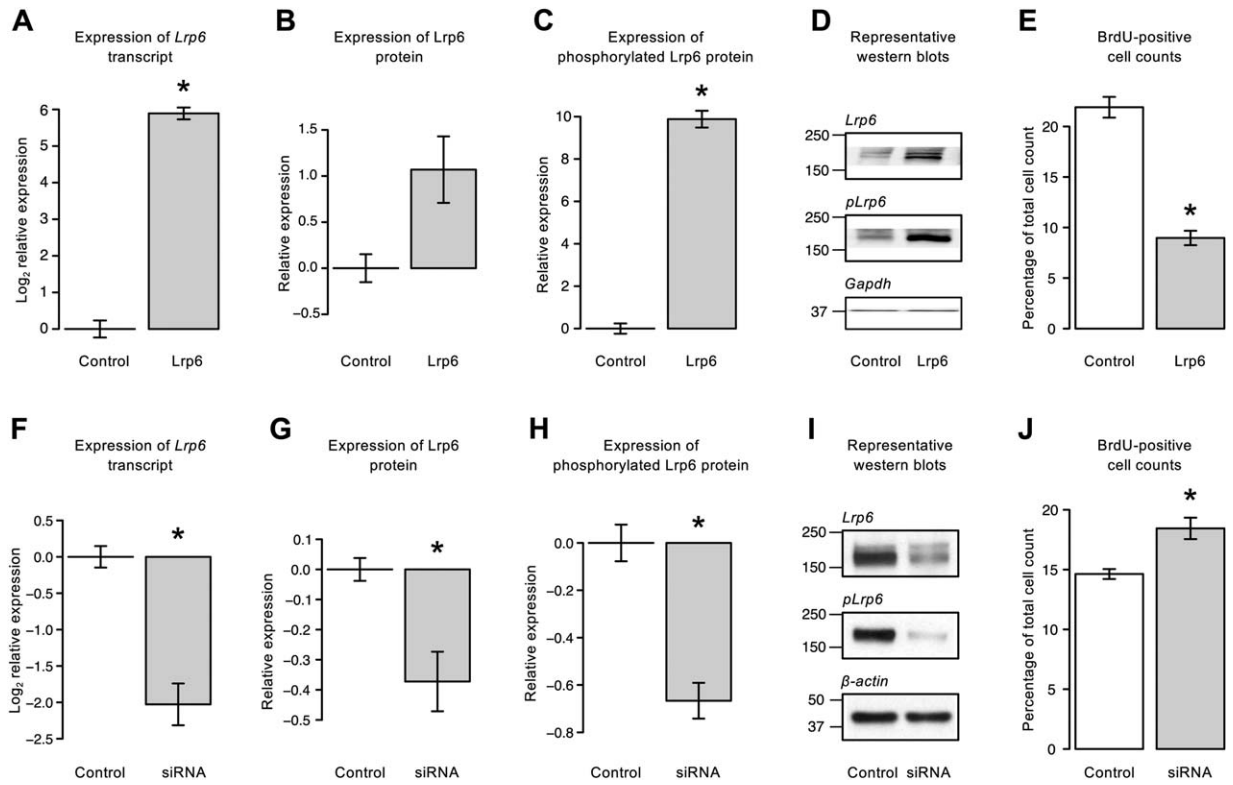

Figure 5. Overexpression and siRNA silencing confirm a negative effect of *Lrp6* on precursor proliferation. Overexpression of a plasmid containing Lrp6 was confirmed by quantitative polymerase chain reaction **(A)** and was shown to lead to an increase in Lrp6 **(B)** and pLrp6 **(C)** levels. Representative Western blots show clear detection of all proteins with the Lrp6 antibody detecting both phosphorylated and nonphosphorylated forms **(D)**. This overexpression resulted in a significant decrease in BrdU incorporation in the proliferating cells in culture **(E)**. Lrp6 transcript expression was also knocked down via siRNA which was confirmed by quantitative PCR **(F)** and Western blot **(G–I)** with a corresponding increase in BrdU incorporation **(J)**. Data are shown as means ± SEM. All changes were significant at $p < .05$ (indicated by asterisks) except for (B) where $p = .052$. Abbreviations: BrdU, 5-bromo-2′-deoxyuridine; siRNA, small interfering RNA.

the *Coa4* gene but did observe *cis*-QTLs for *Lrp6* using different probes from different mircoarray platforms; with a maximum LRS of 27.2 over six probesets targeting exons 2–6; (Affymetrix Exon ST 1.0; GeneNetwork Experiment Accession GN206), an LRS of 49.0 in probe ILM5130064 (Illumina Mouse WG-6 v1.1; GN293) and an LRS of 31.4 from probeset 1451022_at (Affymetrix M430 v2; GN112). The higher mapping power afforded by the larger number of strains in these studies allowed us to confirm that the observed *cis*-QTL for *Lrp6* is indeed real and reproducible. We therefore chose to focus on the candidate *Lrp6* for further validation.

Lrp6 is a Novel Regulator of Adult Hippocampal Precursor Cells

The gene *Lrp6* is located on chromosome 6 and contains 715 single nucleotide polymorphisms. It encodes for a 1,613 amino acid long polypeptide and is known to function in canonical Wnt/β-catenin signaling by acting as a coreceptor with the Frizzled protein [16]. To test the hypothesis that *Lrp6* negatively regulates proliferation of adult hippocampal precursor cells, we performed gain- and loss-of-function experiments in our cell culture model.

To assess the effect of overexpressing *Lrp6* in the proliferating cells, we transfected cells—derived from the parental strain C57BL/6—in suspension by electroporation with a plasmid containing the full-length mouse *Lrp6* coding sequence. We also cotransfected with a plasmid containing *Mesdc2* ("mesoderm development candidate 2") which encodes a molecular chaperone required for the proper folding of Lrp6 and which is necessary for Lrp6 protein maturation and membrane localization [17]. Controls were transfected with the equivalent amount of this plasmid alone. Analysis of *Lrp6* in the cells by qPCR 48 hours after transfection showed an increase in *Lrp6* mRNA ($-\Delta\Delta C_t$, Control: 0 ± 0.23, Lrp6: 5.89 ± 0.16, mean ± SEM; $n = 3$; $t(3.57) = 20.83$, $p = 7.5 \times 10^{-5}$, two-tailed t test; Fig. 5A). We also found an increase in both the nonphosphorylated (NDC, control: 0 ± 0.15, Lrp6: 1.07 ± 0.36, mean ± SEM; $n = 4$; $t(4.03) = 2.73$, $p = .052$, two-tailed t test; Fig. 5B) and phosphorylated (control: 0 ± 0.24, Lrp6: 9.88 ± 0.4, mean ± SEM; $n = 4$; $t(4.96) = 21.36$, $p = 4.5 \times 10^{-6}$, two-tailed t test; Fig. 5C) forms of Lrp6 protein by Western blotting (Fig. 5D), evidence that confirmed successful overexpression. We then measured the proliferation rate of *Lrp6* overexpressing and sham transfected cells by BrdU incorporation. The increased expression of *Lrp6* led to a reduction in the numbers of $BrdU^+$ cells to less than half that seen in the controls (percent of total cell number, control: 21.76 ± 1.12, Lrp6: 8.75 ± 0.98, mean ± SEM; $n = 6$; $t(9.83) = -8.96$, $p = 5.9 \times 10^{-6}$, two-tailed t test; Fig. 5E), indicating that Lrp6 overexpression affects precursor cell proliferation.

We then used siRNA to knock down expression of *Lrp6*. A pool of four siRNAs, or a pool of four nontarget control siRNAs was introduced into adherent cultures using a lipid-based protocol (Materials and Methods section). A fourfold reduction in *Lrp6* mRNA was confirmed by qPCR ($-\Delta\Delta C_t$, control: 0 ± 0.23,

siRNA: -2.01 ± 0.28, mean $\pm$ SEM; $n = 3$; $t(3.86) = -5.53$, $p = .0058$, two-tailed t test; Fig. 5F). Western blotting also showed a reduction in both nonphosphorylated (NDC, control: 0 ± 0.03, siRNA: -0.37 ± 0.07, mean $\pm$ SEM; $n = 3$; $t(2.97) = -5.04$, $p = .015$, two-tailed t test; Fig. 5G) and phosphorylated (NDC, control: 0 ± 0.11, siRNA: -0.67 ± 0.10, mean $\pm$ SEM; $n = 3$; $t(3.91) = -4.53$, $p = .011$, two-tailed t test; Fig. 5H) Lrp6 protein (Fig. 5I). This knockdown of *Lrp6* expression resulted in a modest but significant increase in proliferation as measured by BrdU incorporation (percent of total cell number, control: 14.63 ± 0.41, siRNA: 18.44 ± 0.9, mean $\pm$ SEM; $n = 5$; $t(5.64) = 3.86$, $p = .0094$, two-tailed t test; Fig. 5J). Together, these results confirm the inhibitory role of *Lrp6* on precursor cell proliferation as predicted by the microarray association analysis.

Genes Correlating with Lrp6 Expression Suggest a Role in Cell Cycle Exit

To further use our gene expression resource, we searched for other transcripts among the 21,155 genes represented on the microarray which had similar expression patterns to *Lrp6*. Using a threshold of 0.6, we discovered 98 transcripts with a positive correlation and 144 with a negative correlation to *Lrp6*. A gene ontology enrichment analysis showed that the positive correlates were associated with terms such as "dendrite development," "synapse assembly," and "cell-matrix adhesion" whereas the negative correlates were enriched for "DNA duplex unwinding," "mitotic nuclear division," "chromatin assembly," and "cell division." These results support our conclusion that *Lrp6* expression is a negative regulator of neural precursor cell proliferation in our culture model. A list of the correlating genes as well as the gene ontology results are presented in Supporting Information Tables S1–S4.

Among the most positively correlating genes was *Bdnf* ($r = .72$), known to have a role in differentiation in our cell culture model [18], although the absence of a significant QTL anywhere in the genome argues that this is not directly modulated by genetics but rather is a downstream target of other polymorphic regulators—such as Lrp6. The relationship between Lrp6 and other molecules regulating adult hippocampal precursor proliferation will be an exciting area for further research. The cell and expression resources presented above will be valuable tools in this future work.

Discussion

This study has established a resource of cultured cell lines derived from the hippocampi of different strains of adult mice. In contrast to panels of primary cell preparations, the lines established here are proliferating and, although not immortalized, can be maintained as proliferating cultures over many passages [10]. This means that the same line may be used for many experiments, thus not only vastly reducing the numbers of animals necessary but also increasing reproducibility. As reported here, cellular phenotypes, gene expression assays and gene manipulation experiments may be carried out on the same genetic background—while still harnessing the genetic variance across the different lines. In addition, because the strains used are part of a well-established genetic reference panel, any work with these lines is supported by an enormous body of genomic information, gene expression data and phenotypes. These external resources provide important context.

Our study has exploited the BXD model by measuring rates of proliferation and transcript expression in matched replicate cultures from each of 20 strains and has integrated these data with existing high-density genotypes. This allowed a systems genetics approach in which the proliferation phenotype could be associated with potential regulator genes (identified by the presence of a *cis*-QTL). The most promising candidate from this approach, *Lrp6*, was confirmed to modulate precursor cell proliferation in vitro.

The discovery of a role for *Lrp6* in regulating adult neurogenesis will be a helpful addition to our understanding of this phenomenon, but further studies will be required to elucidate the mechanisms underlying the effect of Lrp6 on proliferation. A central question will be how a role for Lrp6 as a negative regulator of adult neurogenesis might fit into our current understanding of Lrp6 function from other systems. Lrp6 is best known as a Wnt coreceptor in the canonical Wnt signaling pathway [16, 19]. Wnt/β-catenin signaling is initiated by the activation of the frizzled (Fz) receptor, its coreceptor Lrp6, and the cytoplasmic disheveled (Dvl) protein. The promoter region of the basic helix-loop-helix proneural transcription factor NeuroD1 contains regulatory elements that are repressed by Sox2 and activated by the β-catenin/TCF/LEF activator complex following Wnt activation in adult NPCs [20]. Lrp6 binding results in reduced degradation of β-catenin, which in turn translocates into the nucleus to form TCF/LEF transcription activator complexes [21]. In line with this pathway, canonical Wnt signaling positively regulates adult hippocampal neurogenesis [22].

Lrp6, however, is also a specific, high-affinity receptor for the secreted Wnt antagonist Dickkopf 1 (Dkk1) and prevents formation of the Frizzled-Wnt-Lrp6 complex [23]. The polydactyly of Dkk overexpressing ($Dkk1^{d/d}$) mice was corrected by reduced expression of *Lrp6* [24]. Overexpression of Dkk1 massively reduced neurogenesis in the developing hippocampus [25] implying that, dependent on the presence of Dkk1, Lrp6 can have negative or positive effects on Wnt signaling. Neural progenitors with inducible loss of Dkk1 indeed increased their Wnt activity, which led to enhanced self-renewal and increased generation of immature neurons [26]. However, Lrp6 was not specifically analyzed in that study.

In addition, there is a role of Lrp6 in noncanonical Wnt signaling. Lrp6 acts as an inhibitor in planar cell polarity (PCP) signaling in neurulation, which is tightly regulated by a dosage-sensitive balance between the canonical and PCP Wnt pathways [27]. PCP signaling is important for brain development and function, probably including neural stem cell divisions [28]. Finally, the role of Lrp6 is further complicated by the discovery that it can function in different pathways depending on its subcellular localization [29].

The complexity of this picture, which implies that Lrp6 might modulate Wnt activity in more than one way prompted us to end this report with the general confirmation of Lrp6 being able to negatively regulate neural precursor cell proliferation ex vivo. A follow-up study addressing the precise function of Lrp6 in neural stem cells would have to address several large questions: (a) what is the role of canonical versus noncanonical Wnt signaling in neural precursor cells, (b) which ligands are involved and where are they coming from,

(c) what is the genomic basis of the observed strain difference, (d) what are the molecular consequences of this genomic perturbation, and finally (e) can a model be developed that in a mathematically sound way confirms a central role of Lrp6 in the resulting regulatory networks, as suggested by our data. Our current finding reiterates the importance of the Wnt pathway in the regulation of neural precursor proliferation in the adult hippocampus, but cautions that its mechanism may be less clear than we had previously thought.

Although we have investigated only one candidate gene in this study, the transcript expression resource we have deposited online may be used for many other such analyses. With well more than 200 strong *cis*-QTLs waiting to be analyzed, this dataset is already a valuable resource. The power of the panel could be yet further improved, however, by the inclusion of additional lines. While we have shown that 20 lines is sufficient for single gene associations from clearly segregating transcript expression phenotypes, a panel of this size lacks the power to uncover potential multigene effects (epistatic interactions). Also, the ability to directly detect genomic associations from cellular phenotypes (such as proliferation) will be improved in a larger panel. Importantly, new cell lines can simply be added to the existing archive—thereby drastically reducing the number of animals required for phenotyping. Extension of the cell culture panel is currently being undertaken in our laboratory.

The choice to use the BXD genetic reference population for this study means that the phenotypes and expression profiles we have generated can be readily compared with other data from this model. There is an enormous body of phenotype measurements available ranging from other (non-neural) cell cultures to behavior as well as gene expression profiles from 17 different tissues. Indeed, the cell line resource presented here could also be further phenotyped to investigate, for example, expression during differentiation. We have deposited all expression data from this study into the GeneNetwork repository to take full advantage of data-sharing possibilities. It is hoped that cross-experiment comparisons will uncover new relationships between adult hippocampal neurogenesis and as yet unknown regulatory mechanisms.

Conclusion

We have shown in this study that phenotypic measurements (e.g., proliferation) can be integrated with transcript expression and genomic variation to identify candidate phenotype regulators. This approach can also be extended to other combinations of data sources and presents a rich opportunity for further investigation.

Future work will be able to build on the first proof-of-principle findings presented here to further investigate the genetic network surrounding Lrp6. Identification of additional players in this pathway will be essential to understanding the complex regulation of Wnts and their role in controlling neural precursor cell proliferation. The cell culture resource, transcript expression resource, and systems genetics tools described here provide powerful tools to apply to this endeavor.

Acknowledgments

This work was supported by the Helmholtz Virtual Institute GENESYS (German Network of Systems Genetics, VH-VI-242) and SFB 655 “From cells to tissues” (Deutsche Forschungsgemeinschaft).

Author Contributions

S.K. and R.W.O.: conception and design, collection and/or assembly of data, data analysis and interpretation, manuscript writing, and final approval of manuscript; Z.N.: collection and/or assembly of data, manuscript writing, and final approval of manuscript; M.I.: collection and/or assembly of data and final approval of manuscript; G.R.-R.: conception and design and final approval of manuscript; A.G., G.P., and K.S.: collection and/or assembly of data and final approval of manuscript; N.H.: collection and/or assembly of data, financial support, and final approval of manuscript; G.K.: conception and design, financial support, data analysis and interpretation, manuscript writing, and final approval of manuscript.

Disclosure of Potential Conflicts of Interest

The authors indicate no potential conflicts of interest.

References

1 Kempermann G, Jessberger S, Steiner B et al. Milestones of neuronal development in the adult hippocampus. Trends Neurosci 2004;27:447–452.
2 Overall RW, Paszkowski-Rogacz M, Kempermann G. The mammalian adult neurogenesis gene ontology (MANGO) provides a structural framework for published information on genes regulating adult hippocampal neurogenesis. PloS One 2012;7:e48527.
3 Kempermann G, Chesler EJ, Lu L et al. Natural variation and genetic covariance in adult hippocampal neurogenesis. Proc Natl Acad Sci USA 2006;103:780–785.
4 Kempermann G, Kuhn HG, Gage FH. Genetic influence on neurogenesis in the dentate gyrus of adult mice. PNAS 1997;94:10409–10414.
5 Kempermann G, Gage FH. Genetic determinants of adult hippocampal neurogenesis correlate with acquisition, but not probe trial performance, in the water maze task. Eur J Neurosci 2002;16:129–136.
6 Clark PJ, Kohman RA, Miller DS et al. Genetic influences on exercise-induced adult hippocampal neurogenesis across 12 divergent mouse strains. Genes Brain Behav 2011;10:345–353.
7 Taylor BA. Recombinant inbred strains: Use in genetic mapping. In: Morse H III, ed. Origins of Inbred Mice. New York: Academic Press, 1978:423-438.
8 Taylor BA, Wnek C, Kotlus BS et al. Genotyping new BXD recombinant inbred mouse strains and comparison of BXD and consensus maps. Mammalian Genome 1999;10:335–348.
9 Peirce JL, Lu L, Gu J et al. A new set of BXD recombinant inbred lines from advanced intercross populations in mice. BMC Genet 2004;5:7
10 Babu H, Cheung G, Kettenmann H et al. Enriched monolayer precursor cell cultures from micro-dissected adult mouse dentate gyrus yield functional granule cell-like neurons. PLoS One 2007;2:e388.
11 Babu H, Claasen J-H, Kannan S et al. A protocol for isolation and enriched monolayer cultivation of neural precursor cells from mouse dentate gyrus. Front Neurosci 2011;5:89.
12 Dunning MJ, Smith ML, Ritchie ME et al. beadarray: R classes and methods for Illumina bead-based data. Bioinformatics 2007;23:2183–2184.
13 Team R. R: A Language and Environment for Statistical Computing, 2014. Available at: http://www.R-project.org/.
14 Park S-H, Sim Y-B, Kim C-H et al. Role of α-CGRP in the regulation of neurotoxic responses induced by kainic acid in mice. Peptides 2013;44:158–162.
15 Ferraro TN, Golden GT, Smith GG et al. Differential susceptibility to seizures induced by systemic kainic acid treatment in mature

DBA/2J and C57BLl6J mice. Epilepsia 1995; 36:301–307.
16 Tamai K, Semenov M, Kato Y et al. LDL-receptor-related proteins in Wnt signal transduction. Nature 2000;407:530–535.
17 Hsieh JC, Lee L, Zhang L et al. Mesd encodes an LRP5/6 chaperone essential for specification of mouse embryonic polarity. Cell 2003;112:355–367
18 Babu H, Ramírez-Rodríguez G, Fabel K et al. Synaptic network activity induces neuronal differentiation of adult hippocampal precursor cells through BDNF signaling. Front Neurosci 2009;3:49.
19 Pinson KI, Brennan J, Monkley S, et al. An LDL-receptor-related protein mediates Wnt signalling in mice. Nature 2000;407:535–538.
20 Kuwabara T, Hsieh J, Muotri A et al. Wnt-mediated activation of NeuroD1 and retro-elements during adult neurogenesis. Nat Neurosci 2009;12:1097–1105.
21 Niehrs C. Function and biological roles of the Dickkopf family of Wnt modulators. Oncogene 2006;25:7469–7481.
22 Lie DC, Colamarino SA, Song H-J et al. Wnt signalling regulates adult hippocampal neurogenesis. Nature 2005;437:1370–1375.
23 Li Y, Lu W, King TD et al. Dkk1 stabilizes Wnt co-receptor LRP6: Implication for Wnt ligand-induced LRP6 down-regulation. PLoS One 2010;5:e11014.
24 MacDonald BT, Adamska M, Meisler MH. Hypomorphic expression of Dkk1 in the doubleridge mouse: Dose dependence and compensatory interactions with Lrp6. Development 2004;131:2543–2552.
25 Solberg N, Machon O, Krauss S. Effect of canonical Wnt inhibition in the neurogenic cortex, hippocampus, and premigratory dentate gyrus progenitor pool. Dev Dyn 2008; 237:1799–1811.
26 Seib DRM, Corsini NS, Ellwanger K et al. Loss of Dickkopf-1 restores neurogenesis in old age and counteracts cognitive decline. Cell Stem Cell 2013;12:204–214.
27 Allache R, Lachance S, Guyot MC et al. Novel mutations in Lrp6 orthologs in mouse and human neural tube defects affect a highly dosage-sensitive Wnt on-canonical planar cell polarity pathway. Hum Mol Genet. 2014;23:1687–1699.
28 Tissir F, Goffinet AM. Planar cell polarity signaling in neural development. Curr Opin Neurobiol 2010;20:572–577.
29 Beagle B, Johnson GVW. Differential modulation of TCF/LEF-1 activity by the soluble LRP6-ICD. PLoS One 2010;5:e11821.


See www.StemCells.com for supporting information available online.

